The Physics of Space Plasmas

Magnetic Storms and Substorms

William J. Burke
14 November 2012
University of Massachusetts, Lowell

BOSTON COLLEGE ISR INSTITUTE FOR SCIENTIFIC RESEARCH

Lecture 9

- Course term-paper topics
- Geomagnetic Storms: (continued)
  - Volland-Stern Model (details)
    - The ring current's nose structure
    - Stormtime Plumes and Tails
    - Energetic ion local-time distributions
  - Saturation of the cross polar cap potential ➔ Siscoe-Hill model
  - Transmission-line analogy
- Geomagnetic Substorms:
  - Growth-phase phenomenology near geostationary altitude
  - NEXL versus SCW picture: a perennial controversy

Magnetic Storms and Substorms

Term-Paper Topics:

- **The role of $\Delta\Phi_{||}$ in auroral arc formation (phenomenology & theory)**
- **IMF control of dayside cusp locations and dynamics**
- **Region1 – Region 2 control of magnetospheric E-field distributions.**
- **Pitch-angle scattering : Radiation belt "slot" formation**
- **ICMEs and magnetic clouds driving geomagnetic storms**
- **Volland-Stern model: Plume formation and other needed physics**
- **Student/faculty-defined topics**

Magnetic Storms and Substorms

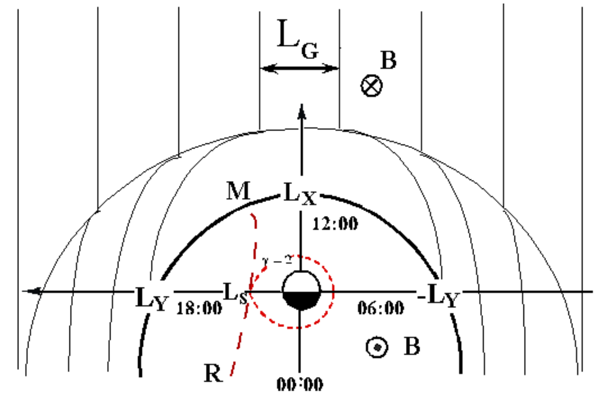

The Volland-Stern single-particle model:

$$\vec{\mathrm{E}}(\mathrm{L},\phi) = -15\left(\frac{mV}{m}\right)\frac{1}{L^2}\left(\left[1-\left(\frac{L}{L_S}\right)^{\gamma+1} Sin\phi\right]\hat{r} - \frac{1}{\gamma}\left(\frac{L}{L_S}\right)^{\gamma+1} Cos\phi\hat{\phi}\right)$$

At the stagnation point L_S the potential is

$$\Phi(L_S,\frac{\pi}{2}) \approx -\frac{91}{L_S}kV\left[1+\frac{1}{\gamma}\right]$$

Since the last closed equipotential touches L_S => calculate locus of this potential

$$\Phi(L_A,\phi) \approx -\frac{91kV}{L_S}\left[1+\frac{1}{\gamma}\right] = -\frac{91kV}{L_A}\left[1+\frac{1}{\gamma}\left(\frac{L_A}{L_S}\right)^{\gamma+1} Sin\phi\right]$$

$$\left(\frac{L_A}{L_S}\right)^{\gamma+1} Sin\phi - \frac{L_A}{L_S}(\gamma+1)+\gamma = 0$$

$$L_A(\phi) = \frac{L_S}{\left[1+\frac{\sqrt{2}}{\gamma}\left|Cos\left(\frac{\phi-3\pi/2}{2}\right)\right|\right]}$$

- **$L_A(\phi)$ gives shape of zero-energy Alfvén boundary (ZEAB)**
- **Still don't know what γ means or how to relate E_M to the interplanetary medium.**

The Volland-Stern single-particle model:

At the magnetopause on the dawn (L_Y, 3π/2) and dusk (L_Y, π/2) the potentials are approximately $\Phi_{PC}/2$ and - $\Phi_{PC}/2$, respectively.

$$\Phi_M(L_Y,\frac{\pi}{2}) = -\frac{91kV}{\gamma L_Y}\left(\frac{L_Y}{L_{S\gamma}}\right)^{\gamma+1} = -\frac{\Phi_{PC}(kV)}{2}$$

$$L_{S\gamma} = L_Y\left[\frac{182}{\gamma L_Y \Phi_{PC}(kV)}\right]^{\frac{1}{\gamma+1}}$$

$$\Phi(L,\phi) = -\frac{91kV}{L} - \frac{\Phi_{PC}(kV)}{2}\left(\frac{L}{L_Y}\right)^{\gamma} Sin\phi$$

$$\vec{\mathrm{E}}(\mathrm{L},\phi) = -\frac{91(kV)}{R_E L^2}\hat{R} + \frac{\Phi_{PC}(kV)}{2R_E L_Y}\left(\frac{L}{L_Y}\right)^{\gamma-1}\left[\gamma Sin\phi\hat{R} + Cos\phi\hat{\phi}\right]$$

Average *E* across magnetosphere $\leq$ **1** $\hat{Y}$

$L_Y \approx 1.5\ L_X$

$$L_X \approx \sqrt[6]{\frac{B_0^2}{\mu_0 P_{SW}}} \approx \frac{9.6}{\sqrt[6]{P_{SW}(nPa)}}$$

$$L_Y \approx 14.4/\sqrt[6]{P_{SW}(nPa)}$$

Magnetic Storms and Substorms

ZEAB shape normalized to L_S.
Last closed equipotential of a vacuum field model, <u>not</u> the plasmapause.

L_S as function of Φ_{PC} for P_{SW} = 1, 10 *nPa*

$$\frac{L_A(\phi)}{L_S} = \left[1 + \frac{\sqrt{2}}{\gamma}\left|Cos\left(\frac{\phi - 3\pi/2}{2}\right)\right|\right]^{-1}$$

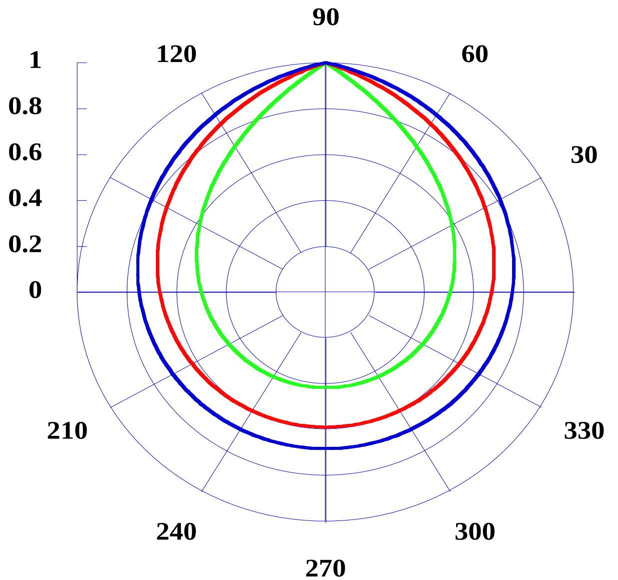

γ = 1, 2, 3

$$L_{S\gamma} = L_Y\left[\frac{182}{\gamma L_Y \Phi_{PC}(kV)}\right]^{\frac{1}{\gamma+1}} = L_Y^{\frac{\gamma}{\gamma+1}}\left(182/\gamma\Phi_{PC}\right)^{\frac{1}{\gamma+1}}$$

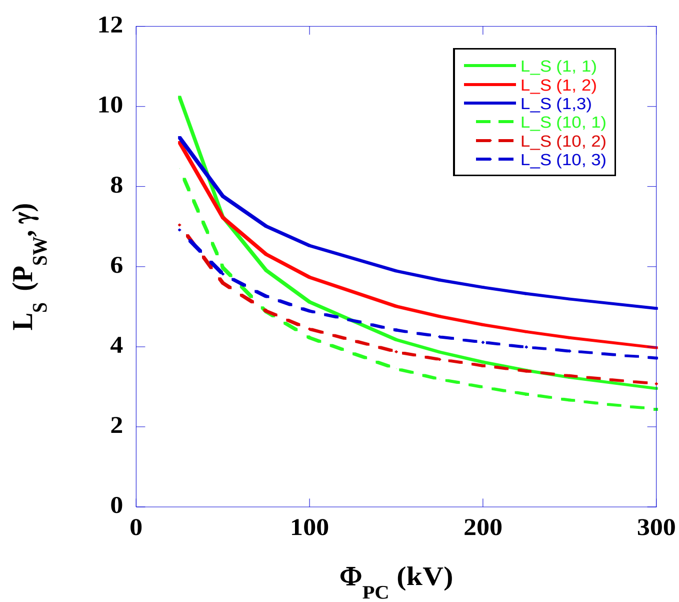

Magnetic Storms and Substorms

- Consider a simple example in which the dynamic pressure of the solar wind P_{SW} and cross polar cap potential Φ_{PC} rise from 1 to 10 nPa and from 50 to 150 kV while γ decreases from 3 to 1.

- Consequently the ZEAB and the separatrix equipotentials move Earthward.

- Cold plasma between the old and new ZEAB finds itself on open equipotentials where it forms the stormtime magnetospheric plume.

- There is a conceptual difference between the ZEAB and the plasmapause.

- Plumes observed by IMAGE limited by intensity of resonant 517 Å scattering by cold He^+ ions.

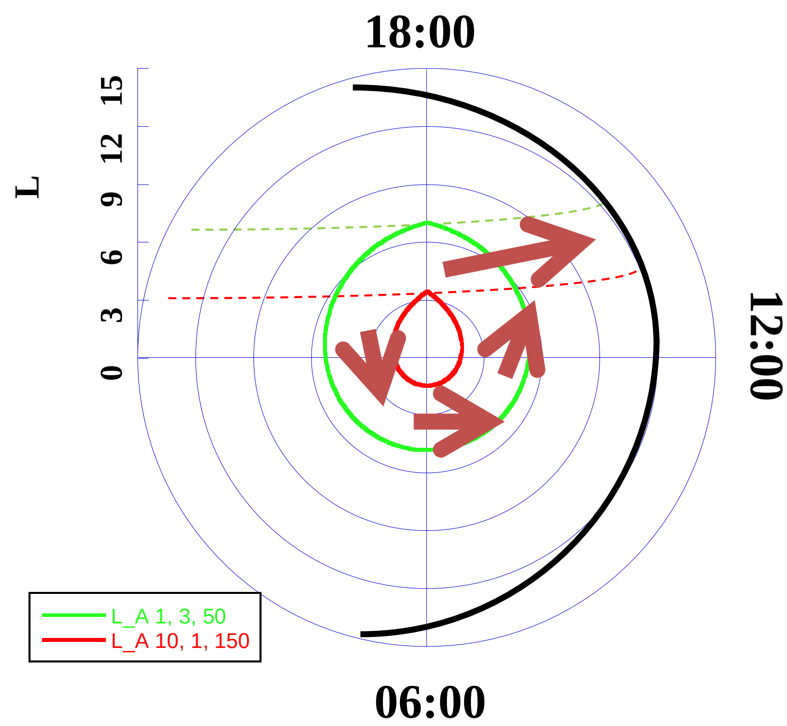

Magnetic Storms and Substorms

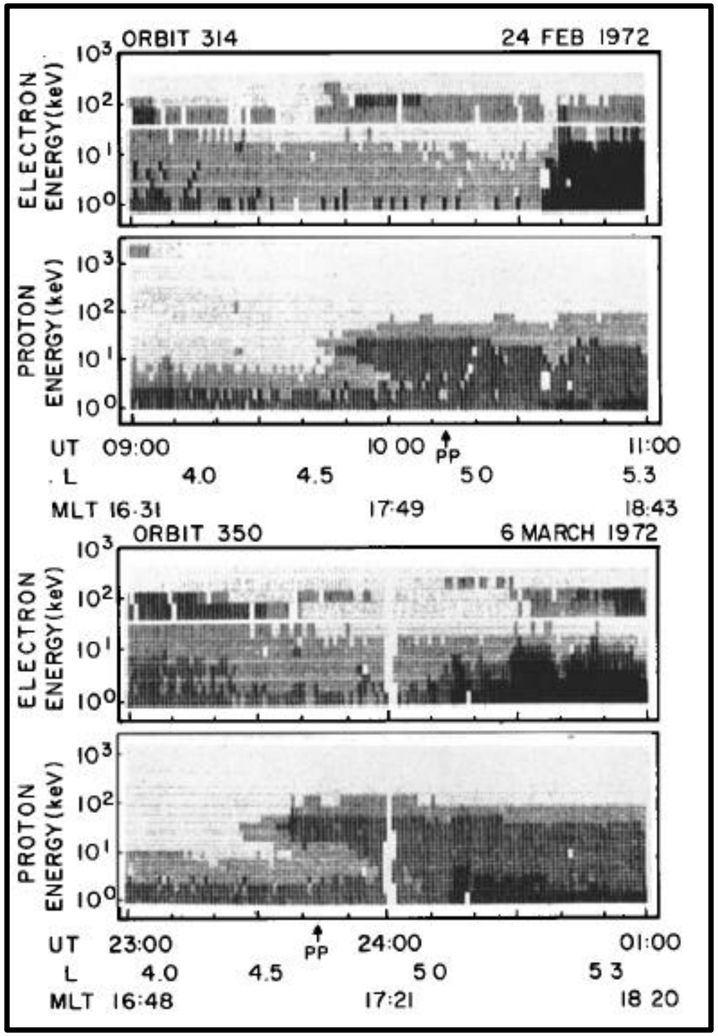

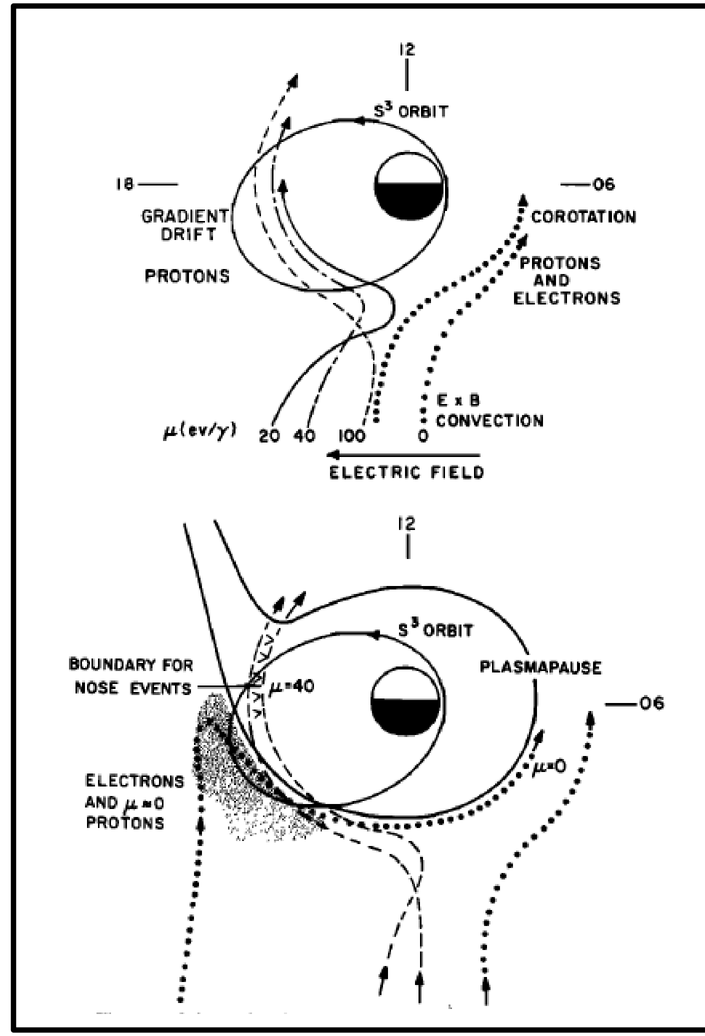

Smith and Hoffman, *JGR, 79*, 966 – 971, 1974.

Magnetic Storms and Substorms

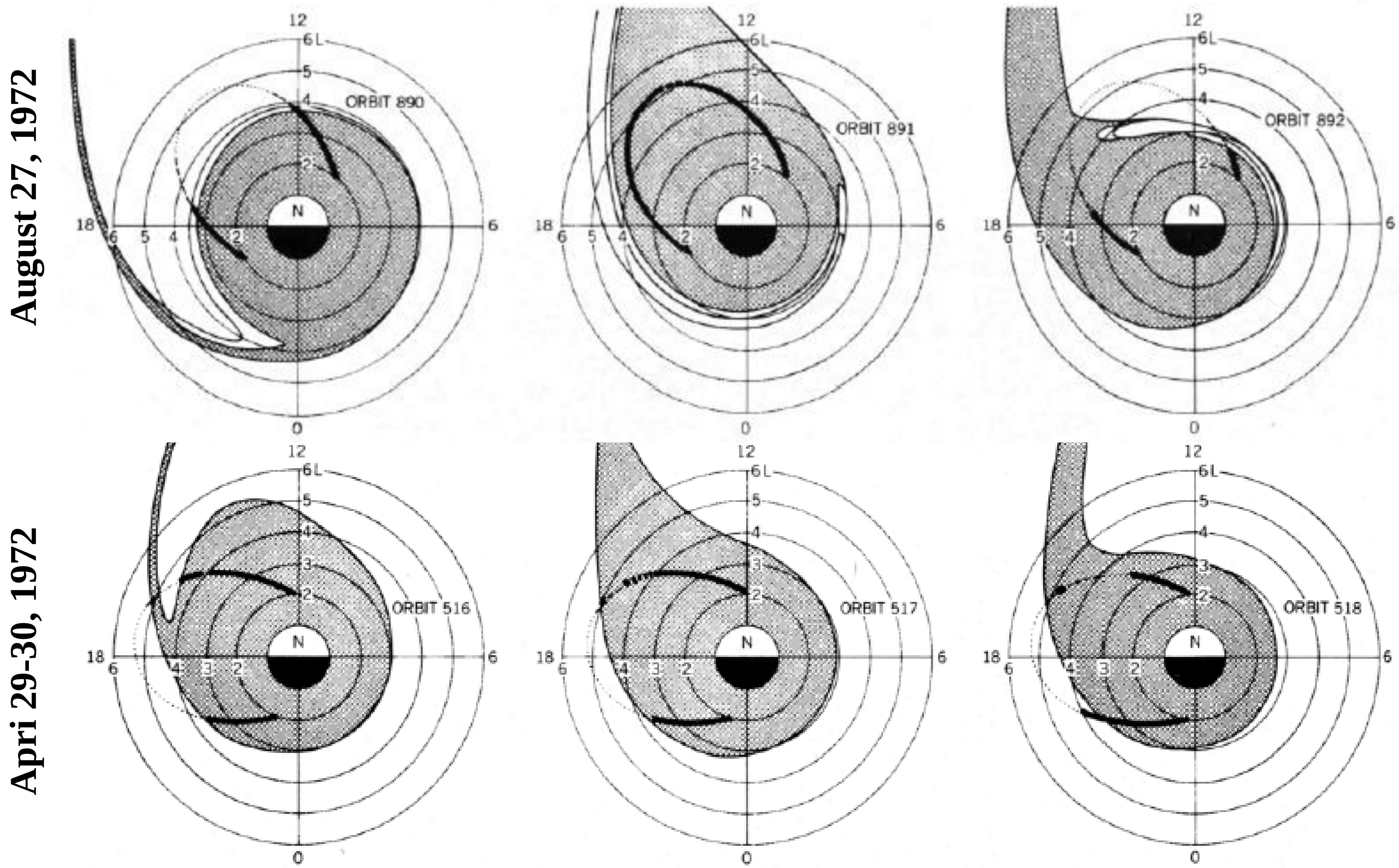

Maynard and Chen, JGR, 80, **1009 – 1013, 1975**

Magnetic Storms and Substorms

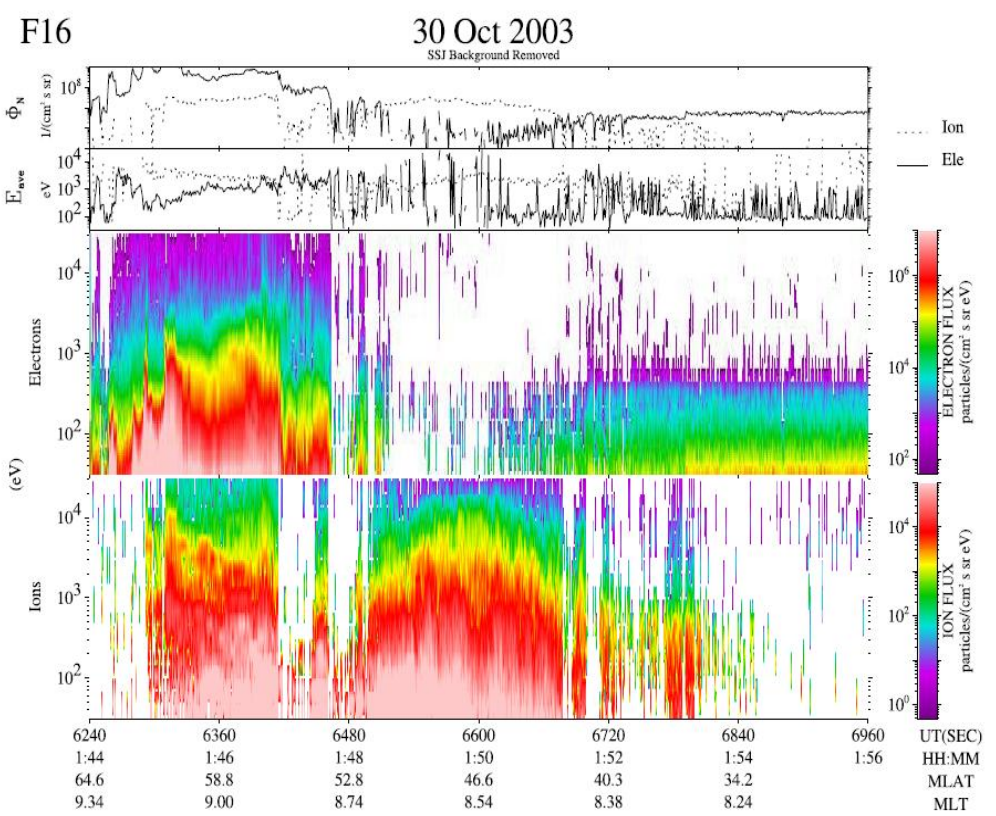

In the previous lecture on magnetic-storm phenomenology we noted that during the recovery phase the ring current becomes more symmetric:

- ***Tsyganenko and Sitov* (2005)**
- ***Love and Gannon* (2010)**

- **Cheryl Huang noticed that during the recovery phase of large storms DMSP was detecting large fluxes of precipitating ions in the dawn MLT sector, at latitudes well equatorward of the auroral electron boundary.**

- **We used a time-dependent version of the Volland-Stern model to try to explain this unexpected phenomenon.**

Huang, C. Y., W. J. Burke, and C. S. Lin, Low-energy ion precipitation during the Halloween storm, *J. Atmos. Solar-Terr. Phys.*, *69*, 101-108, 2007.

Magnetic Storms and Substorms

CRRES Orbit 589 during early recovery phase of March 1991 storm.

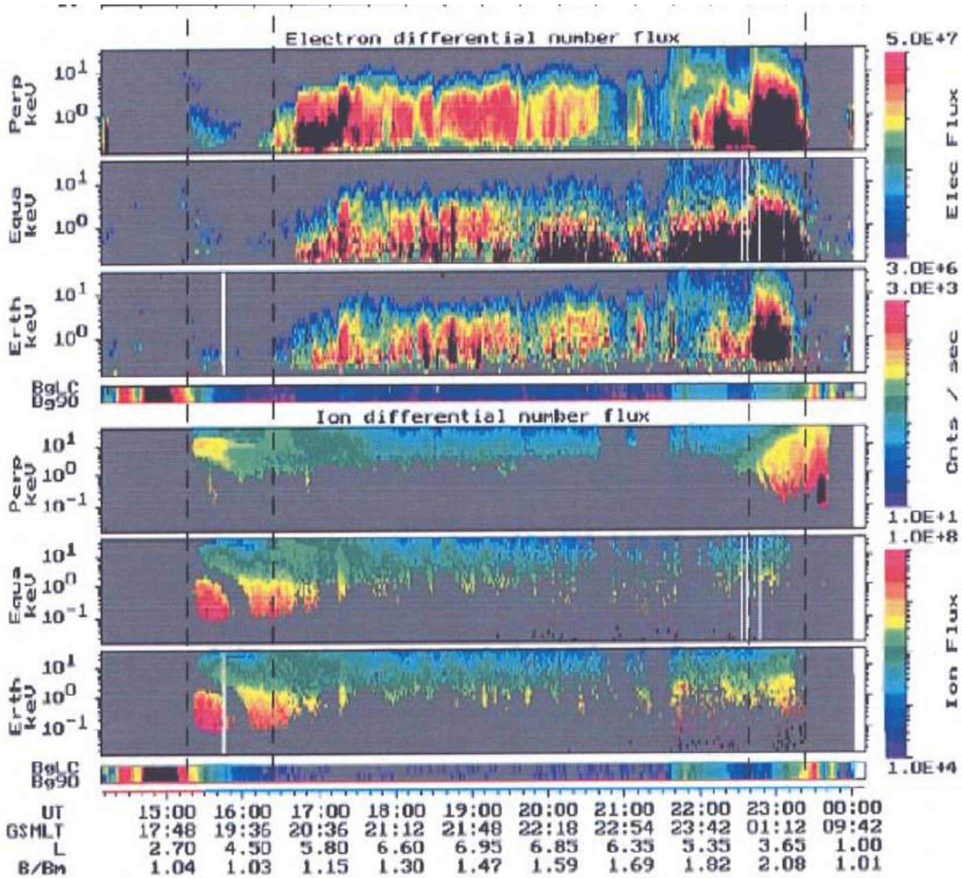

V-S simulation inputs

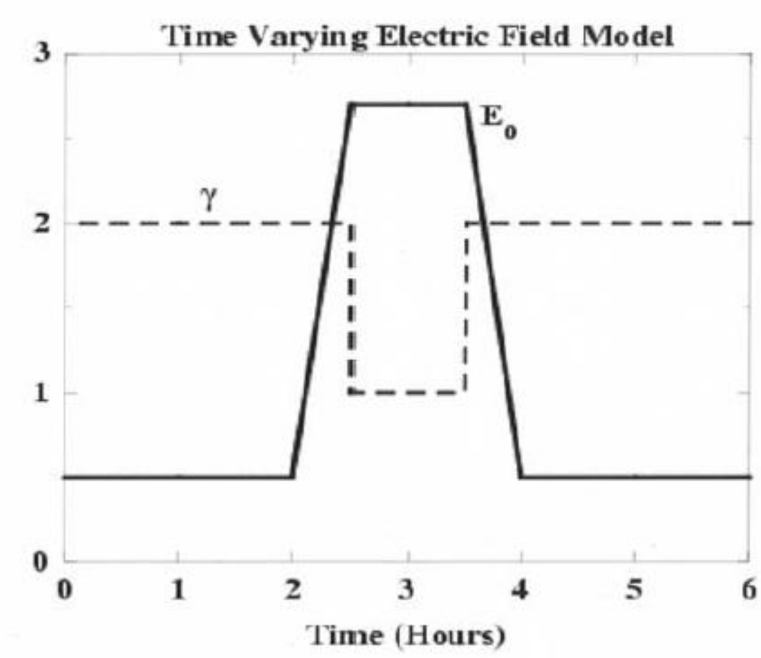

Magnetic Storms and Substorms

$$L_A(\pi) = L_S \Big/ \left(1 + \frac{2}{\gamma}\right)$$

$$\vec{V}_{Vor}(m/s) = \Omega_E R_E L \hat{\phi}$$

$$\vec{V}_{Grad}(m/s) = \frac{\mu}{qB^2} \vec{B} \times \nabla B = -\frac{3\mu}{qR_E L} \hat{\phi}$$

$$\mu_C = \frac{q\Omega R_E^2 L_A^2(\pi)}{3} = \frac{q\Omega R_E^2 L_S^2}{3\left(1 + \frac{2}{\gamma}\right)^2}$$

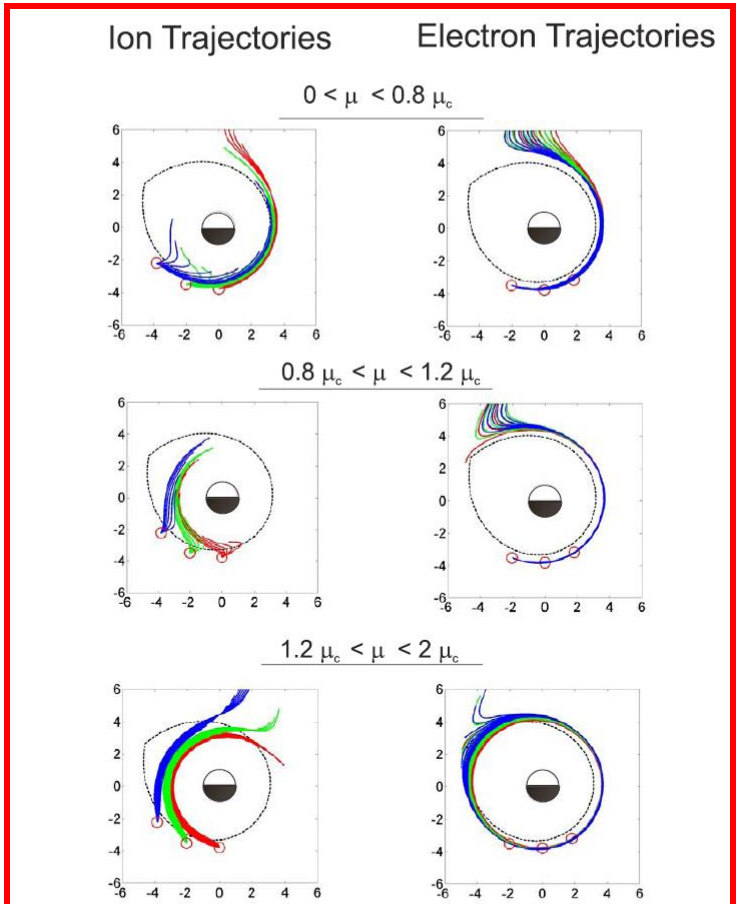

Figure 9. Ion and electron trajectories representative of the lull phase with a constant uniform dawn-to-dusk electric field $E_0 = 0.5$ mV/m. Ion trajectories are shown in the left three panels, and electron trajectories are presented in the right panels for three different ranges of magnetic moment μ. In each panel particle trajectories from three different initial points are represented in three colors. Ion trajectories are shown for three initial points: 2000, 2200, and 2400 hours LT at 4.3 R_E, whereas electron trajectories are shown for three initial points: 2200, 2400, and 0200 hours LT at 4.3 R_E. Eight trajectories are plotted from each initial point for particles with magnetic moments evenly separated by 0.1 μ_c in the range appropriate for the various panels.

Magnetic Storms and Substorms

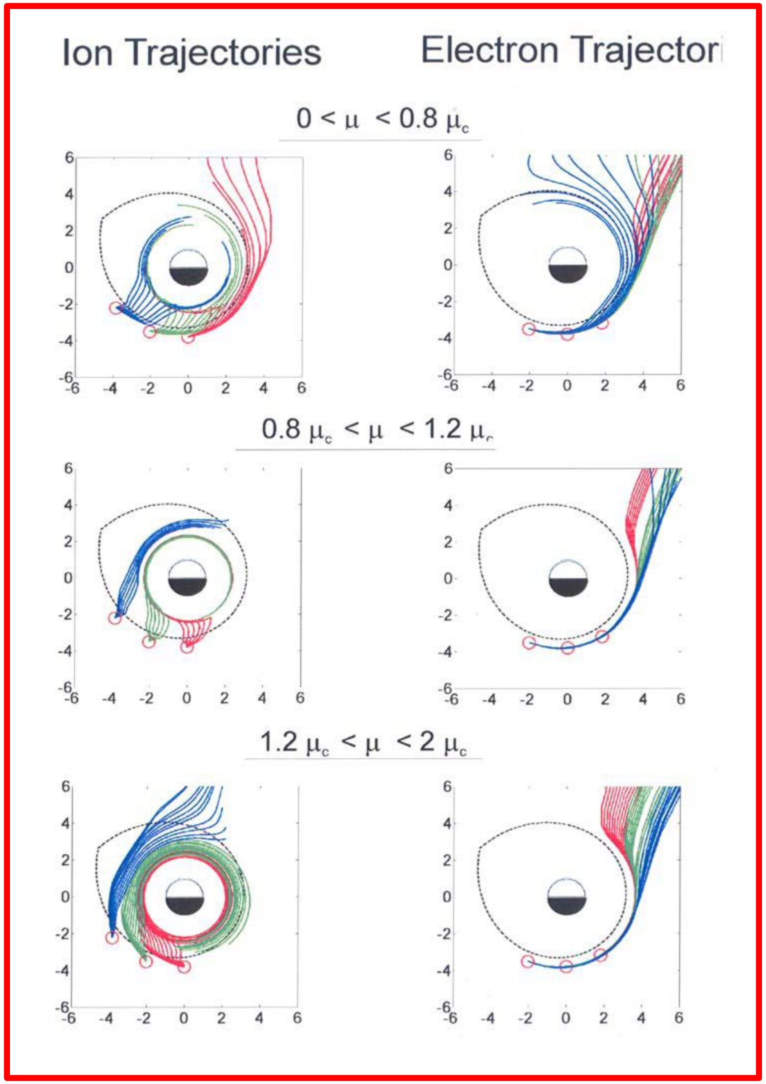

Main-phase electric field period.

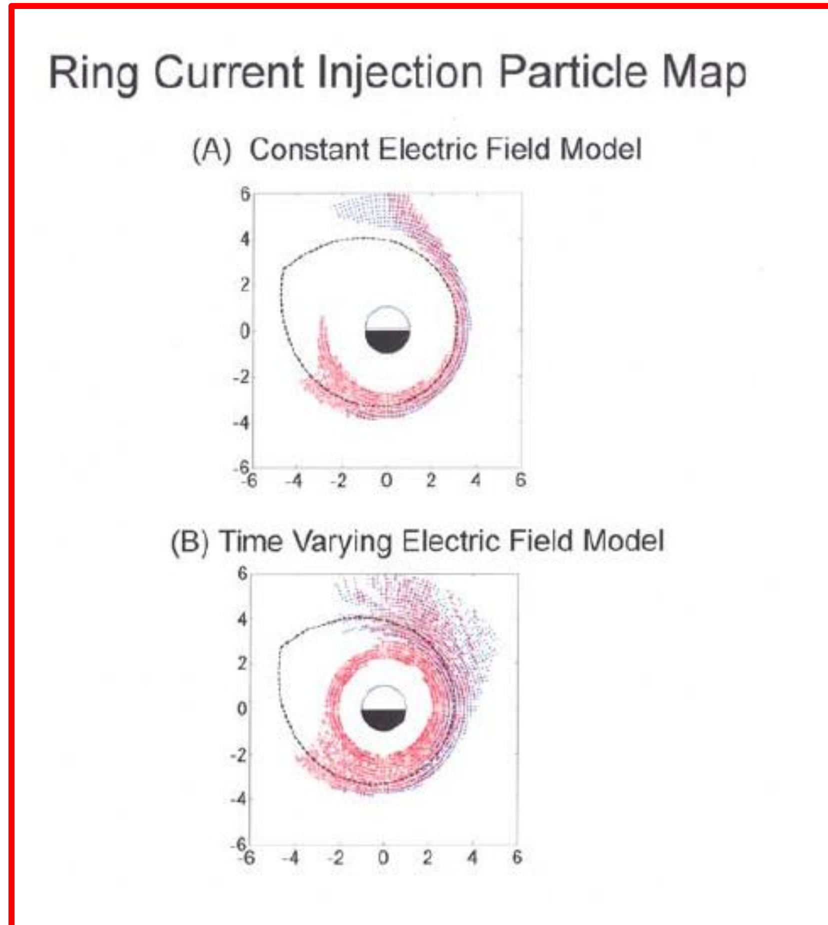

Figure 12. Locations of ions (red) and electrons (blue) with $\mu < 2\mu_c$ in the equatorial plane after drifting for six hours, as predicted by the steady and time-varying electric field models. As in Figure 9, the constant electric field model (A) held $E_0 = 0.5$ mV/m. The time-varying model (B) used the E_0 and γ profiles of Figure 10. Ion (electron) initial positions were evenly distributed in MLT from 2000 (2200) to 2400 (0200).

Magnetic Storms and Substorms

A reminder of innocent but happy times

Independent studies using AE-C, S3.2 and DE-2 measurements of Φ_{PC} all showed that the highest correlation was obtained with

LLBL potential **IEF**

$$\Phi_{PC}(kV) = \Phi_0(kV) + \alpha V_{SW} B_T Sin^2(\theta/2)$$

$$B_T = \sqrt{B_Y^2 + B_Z^2}$$

$$\theta = B_Z / B_T$$

- **Interplanetary electric field (IEF) in mV/m. Since 1 mV/m $\approx$ 6.4 kV/ R_E**
- **L_G => width of the gate in solar wind (~ 3.5 R_E) through which geoeffective streamlines flow.**

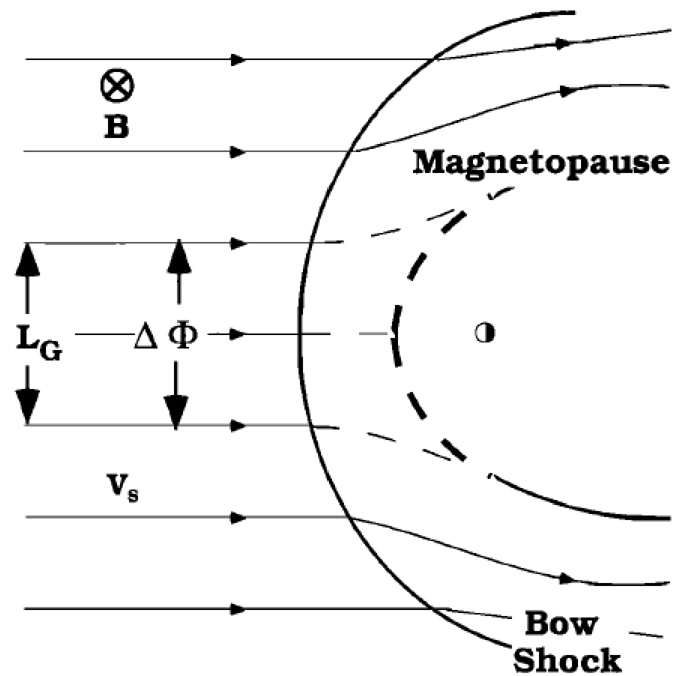

Burke, Weimer and Maynard, **JGR, 104, 9989, 1999.**

Then the Bastille Day storm happened

Magnetic Storms and Substorms

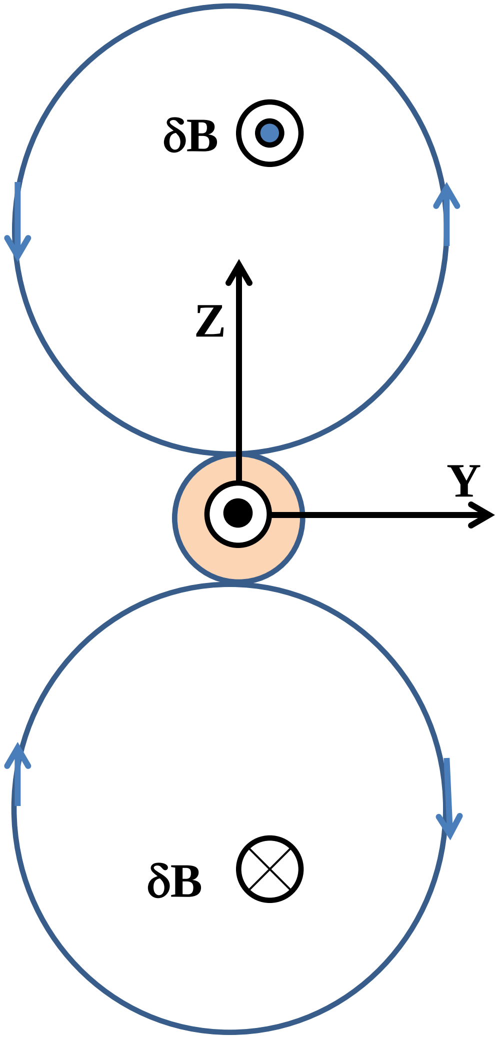

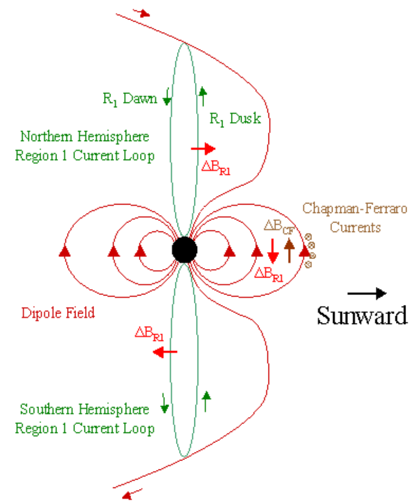

Model validation with F13 & F15

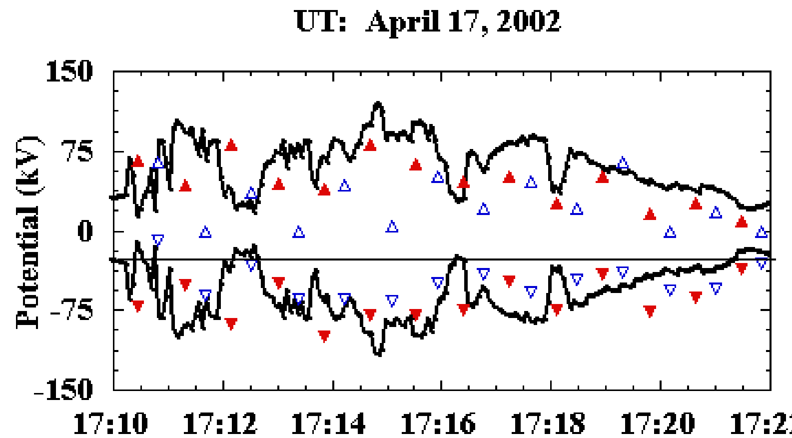

$$\Phi_{PC} = \Phi_I \Phi_S / (\Phi_I + \Phi_S)$$

$$\Phi_I = \Phi_0 + \Lambda_G V B_T \sin^2(\theta/2)$$

$$\Phi_S = 1600 P_{SW}^{0.33} (\text{nPa}) / \Sigma$$

Siscoe et al. (2002), Hill model of transpolar saturation: Comparisons with MHD simulations, *JGR 107*, A6, 1025.

Ober et al. (2003), Testing the Hill model of transpolar potential saturation, *JGR*, *108*, (A12),

MRC: ISM Simulations with IMF B_Z = -2 and -20 nT

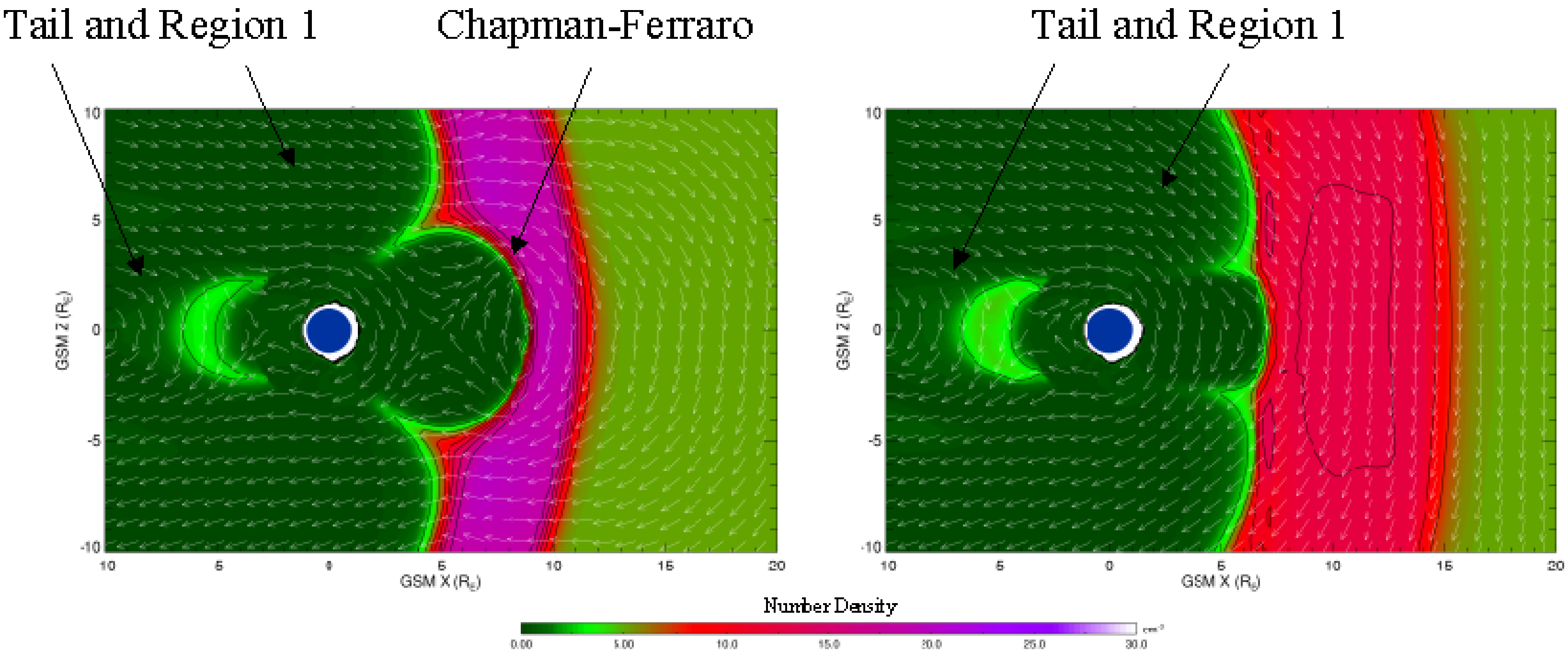

Noon-midnight cross section of the magnetosphere showing the direction of the magnetic field produced by the Chapman-Ferraro, region 1, and tail current systems.

Effects of Region 1 turn-on near main-phase onset

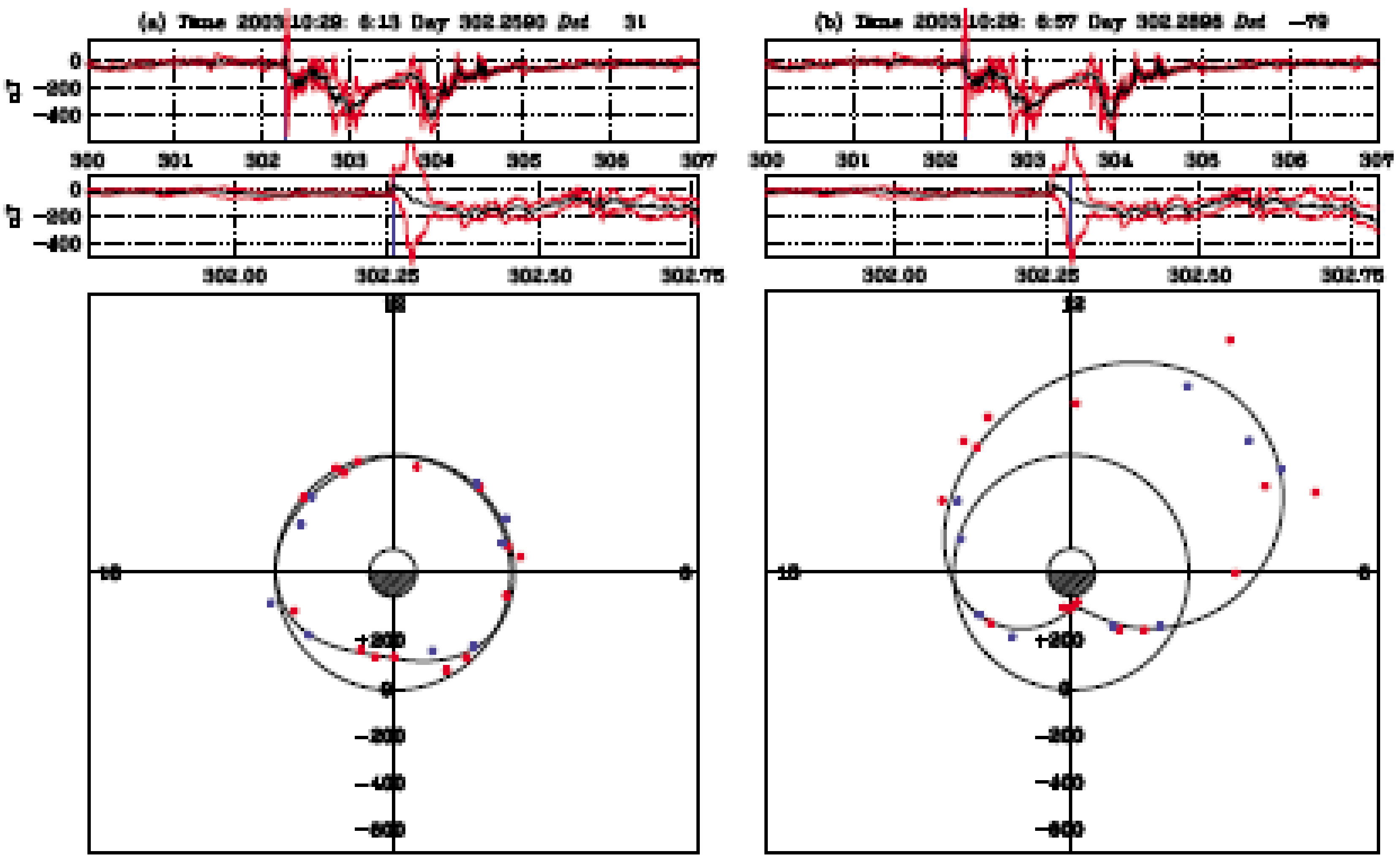

Magnetic Storms and Substorms

During the late main phase of the April 2000 magnetic storm multiple DMSP satellites observed large amplitude FACs with $\Delta\delta B > 1300$ nT).

Associated electric fields on the night side were very weak suggesting relatively large $\Sigma_P > 30$ mho.

No commensurate ΔH measured on ground => Fukushima's theorem?

Do precipitating ions play a significant role in creating and maintaining Σ_P? [*Galand and Richmond*, JGR, 2001]

Huang, C. Y., and W. J. Burke, Transient sheets of field-aligned current observed by DMSP during the main phase of a magnetic storm, *J. Geophys. Res.*, *109*, 2004.

Magnetic Storms and Substorms

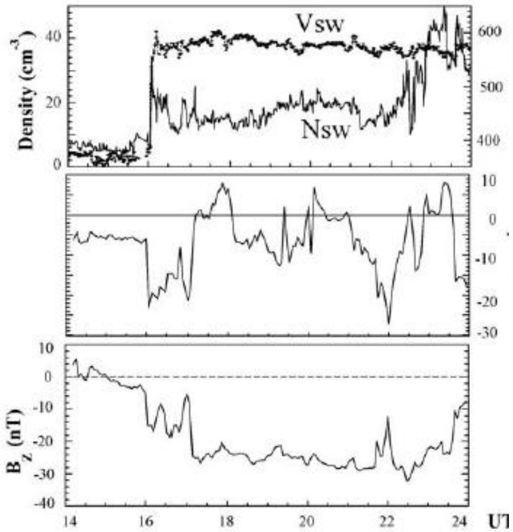

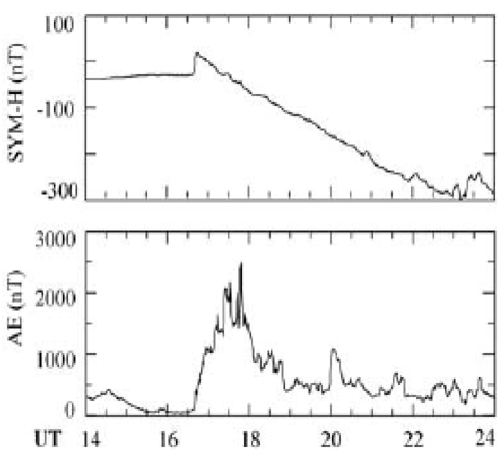

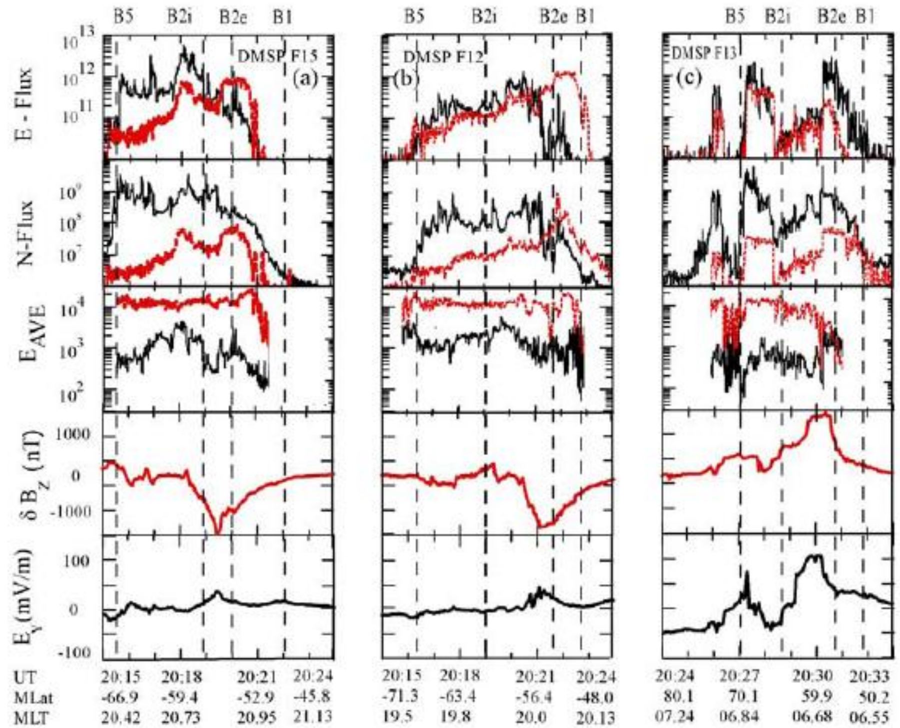

$$\partial_Y [\delta B_Z - \mu_0 (\Sigma_P E_Y - \Sigma_H E_Z)] = 0$$

$$\Sigma_P \approx (1/\mu_0) [\Delta \delta B_Z / \Delta E_Y].$$

Huang, C. Y. and W. J. Burke (2004) Transient sheets of field-aligned currents observed by DMSP during the main phase of a magnetic superstorm, *JGR, 109*, A06303.

Magnetic Storms and Substorms

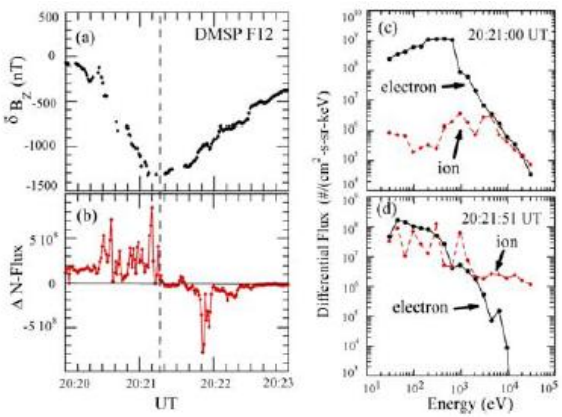

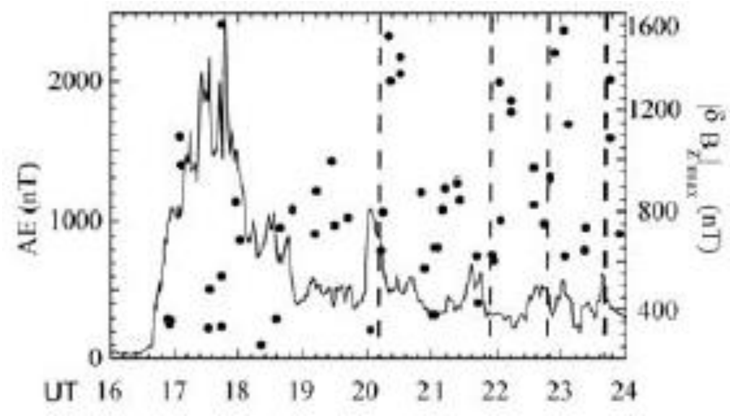

<u>Transmission line model</u>

$$E_Y = E_{Yi} + E_{Yr} \Rightarrow E_{Yr} = RE_{Yi}$$

$$R = \frac{\Sigma_A - \Sigma_P}{\Sigma_A + \Sigma_P}$$

$$\Sigma_A = 1/\mu_0 V_{AR}$$

$$B_Z = B_{Zi} + B_{Zr}$$

$$\frac{E_{Yi}}{\delta B_{Zi}} = V_{AS} = -\frac{E_{Yr}}{\delta B_{Zr}} = -\frac{RE_{Yi}}{\delta B_{Zr}}$$

$$\delta B_{Zr} = -R\delta B_{Zi}$$

$$\frac{\delta B_Z}{E_Y} = \frac{\delta B_{Zi} + \delta B_{Zr}}{E_{Yi} + E_{Yr}} = \frac{1}{V_{AS}}\frac{1-R}{1+R} = \frac{1}{V_{AS}}\frac{\Sigma_P}{\Sigma_A} = \frac{V_{AR}}{V_{AS}}\mu_0\Sigma_P$$

<u>“Measured” Poynting Flux</u>

$$S_{\parallel} = \frac{\vec{E}_Y \times \delta\vec{B}_Z}{\mu_0} = \frac{E_Y \delta B_Z}{\mu_0}(1-R^2) = S_{\parallel i}(1-R^2) = S_{\parallel i} - S_{\parallel r}$$

V_{AR} = Alfvén speed in reflection layer

V_{AS} = Alfvén speed at satellite location

Magnetic Storms and Substorms

Growth phases occur in the intervals between southward turning of IMF B_Z and expansion-phase onset. They are characterized by:

- **Slow decrease in the H component of the Earth's field at auroral latitudes near midnight.**
- **Thinning of the plasma sheet and intensification of tail field strength.**

We consider growth phase electrodynamics observed by the CRRES satellite near geostationary altitude in the midnight sector.

- **McPherron, R. L., Growth phase of magneto-spheric substorms, *JGR, 75*, 5592 – 5599, 1970.**
- **Lui, A. T. Y., A synthesis of magnetospheric substorm models, *JGR, 96*, 1849, 1991.**
- **Maynard, et al., Dynamics of the inner magnetosphere near times of substorm onsets, JGR, 101, 7705 - 7736, 1996.**
- **Erickson et al., Electrodynamics of substorm onsets in the near-geosynchronous plasma sheet, *JGR, 105*, 25,265 – 25,290, 2000.**

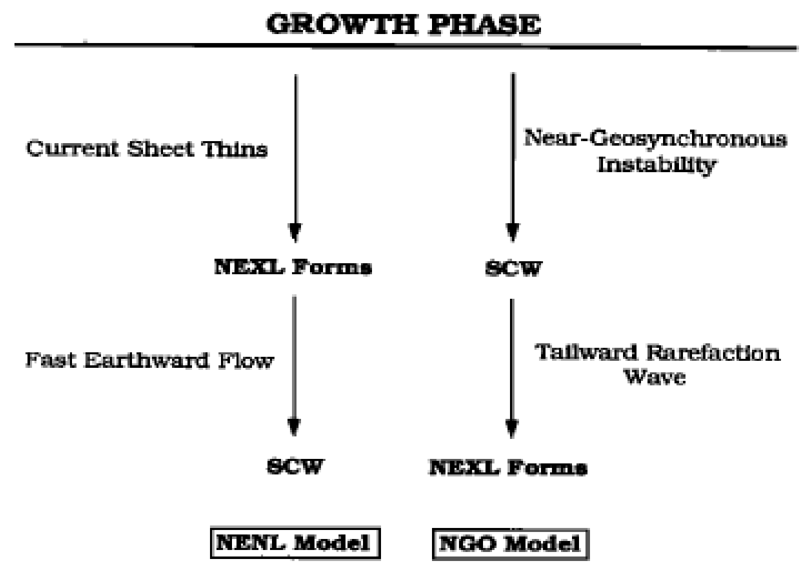

Figure 1. The causal link between near-Earth X line (NEXL) formation and the substorm current wedge (SCW) within the two substorm hypotheses: (left) the near-Earth neutral line (NENL) model and (right) the near-geosynchronous onset (NGO) model.

Magnetic Storms and Substorms

CRRES measurements near local midnight and geostationary altitude during times of isolates substorm growth and expansion phase onsets

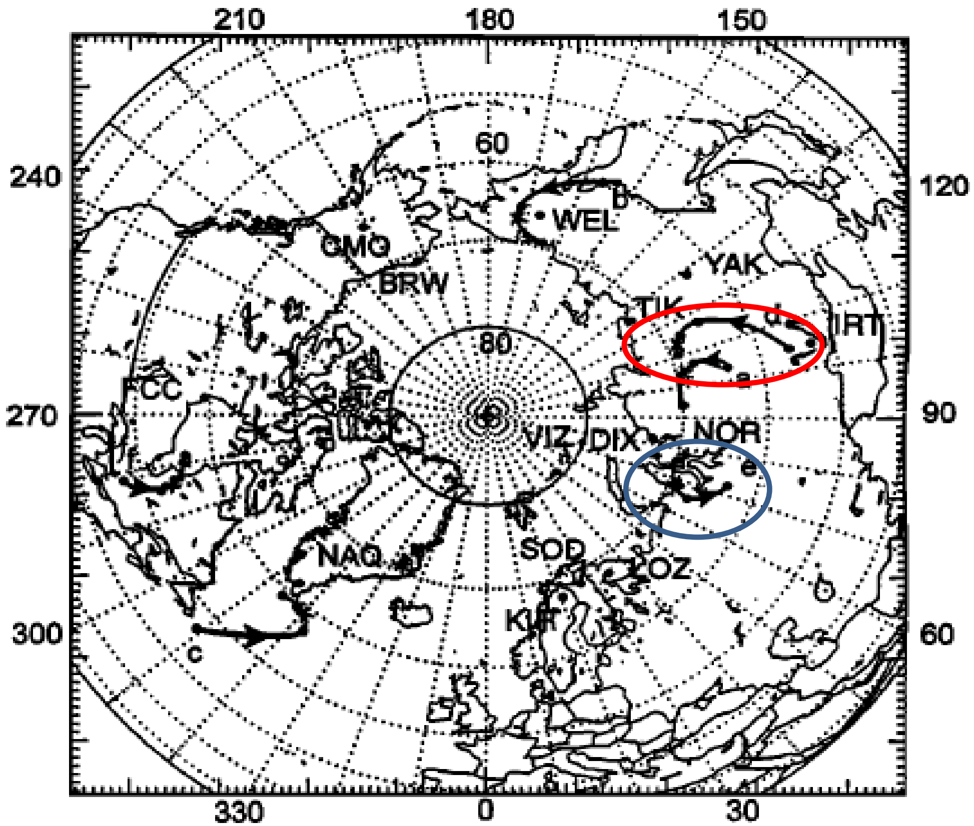

Ionospheric footprints of CRRES trajectories during orbits 535 (red) and 540 (blue).

Magnetic Storms and Substorms

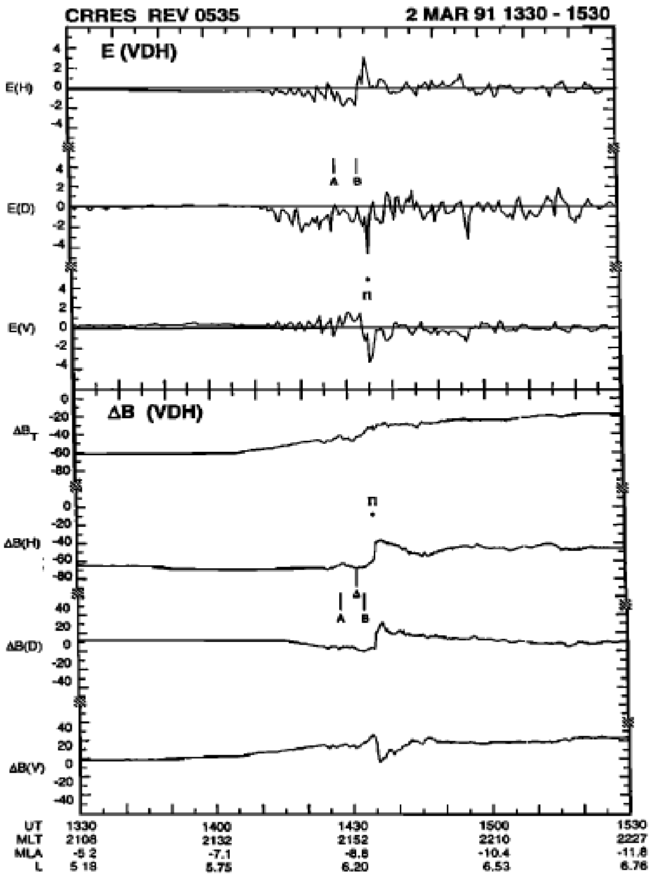

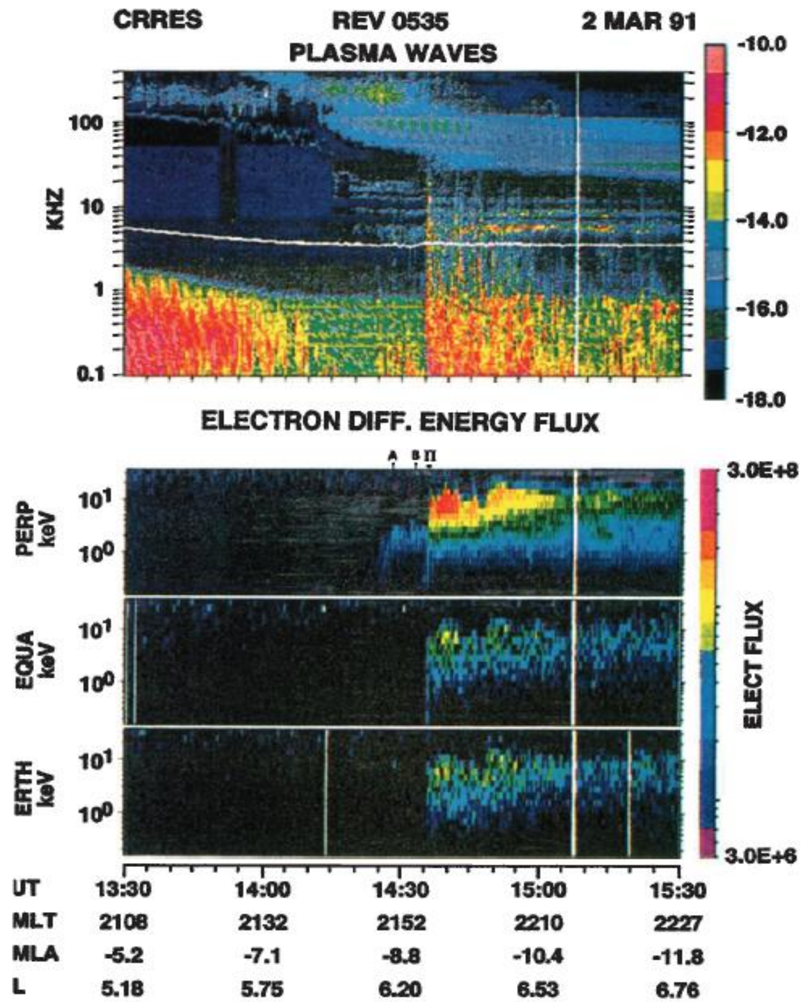

Magnetic Storms and Substorms

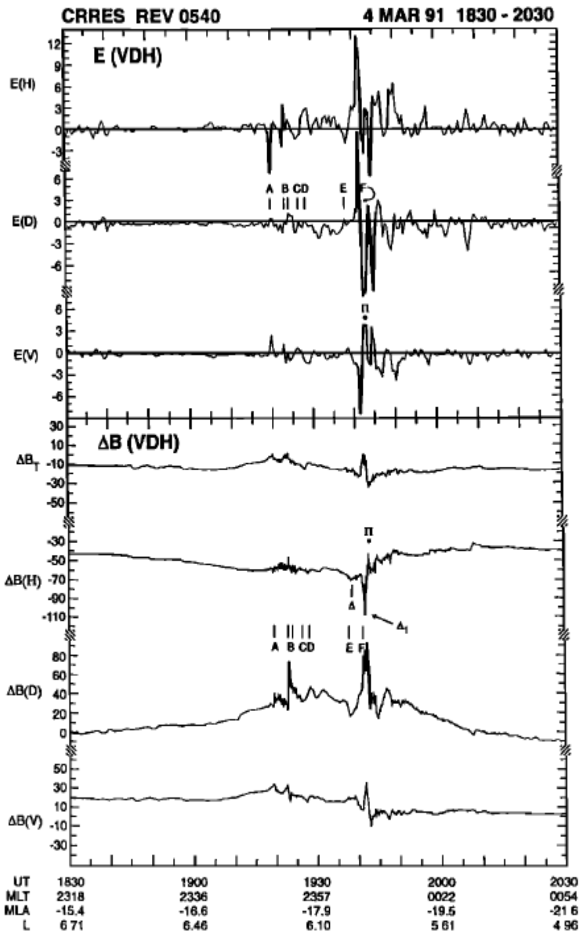

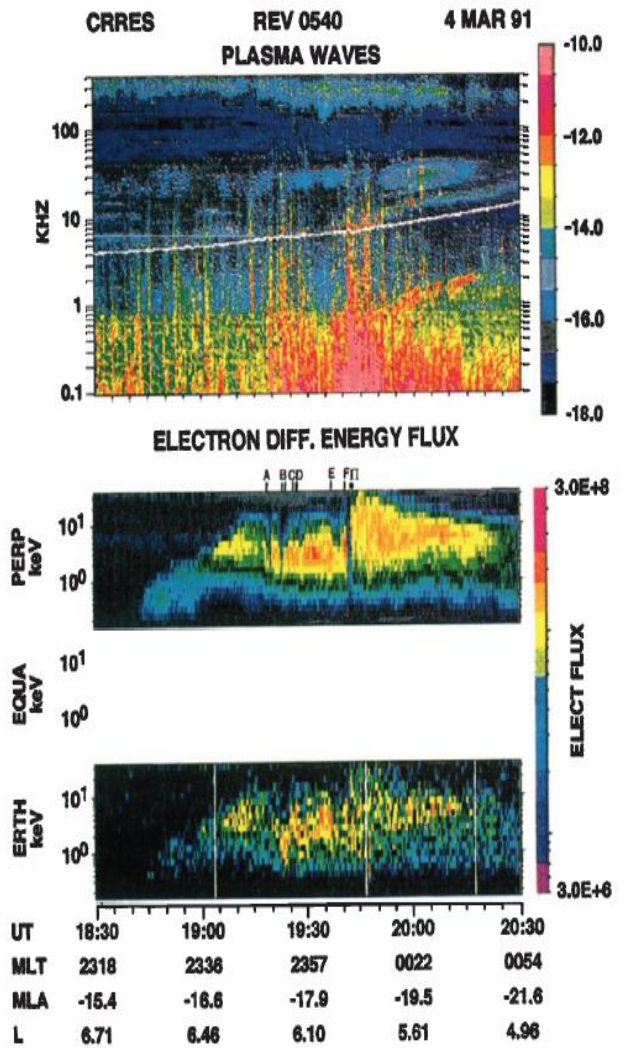

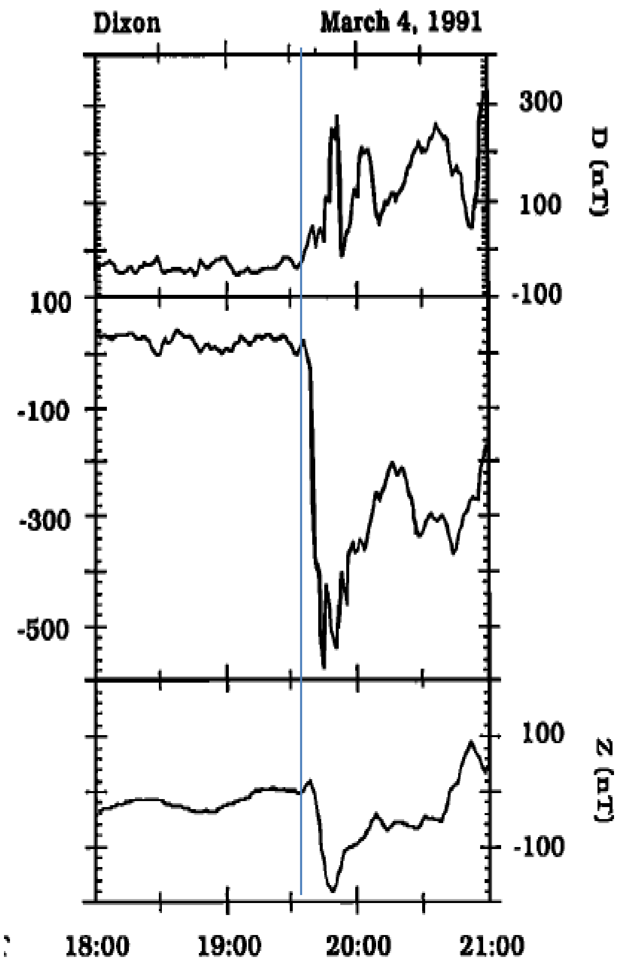

Magnetic Storms and Substorms

Erickson et al., JGR 2000: Studied 20 isolated substorm events observed by CRRES. We will summarize one in which the CRRES orbit (461) mapped to Canadian sector

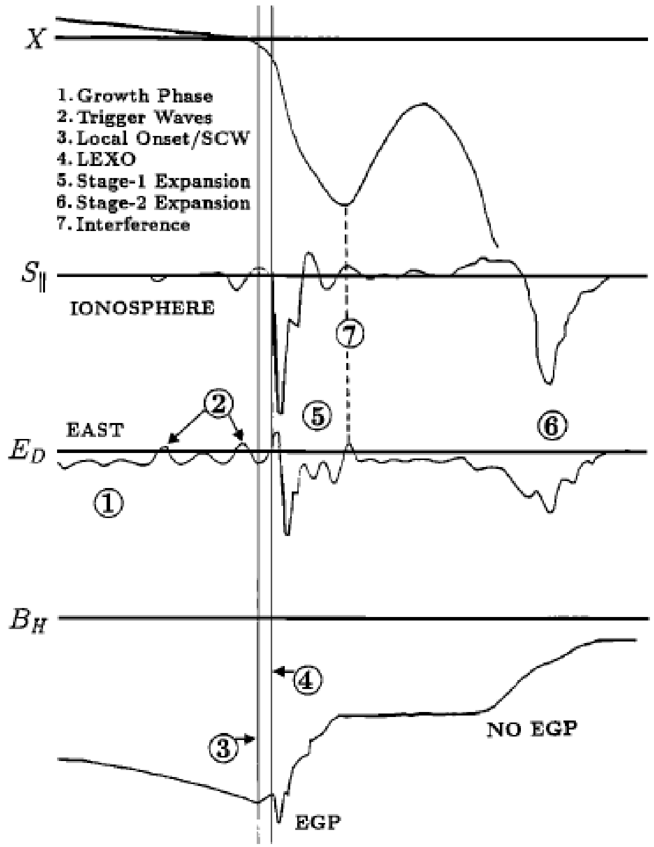

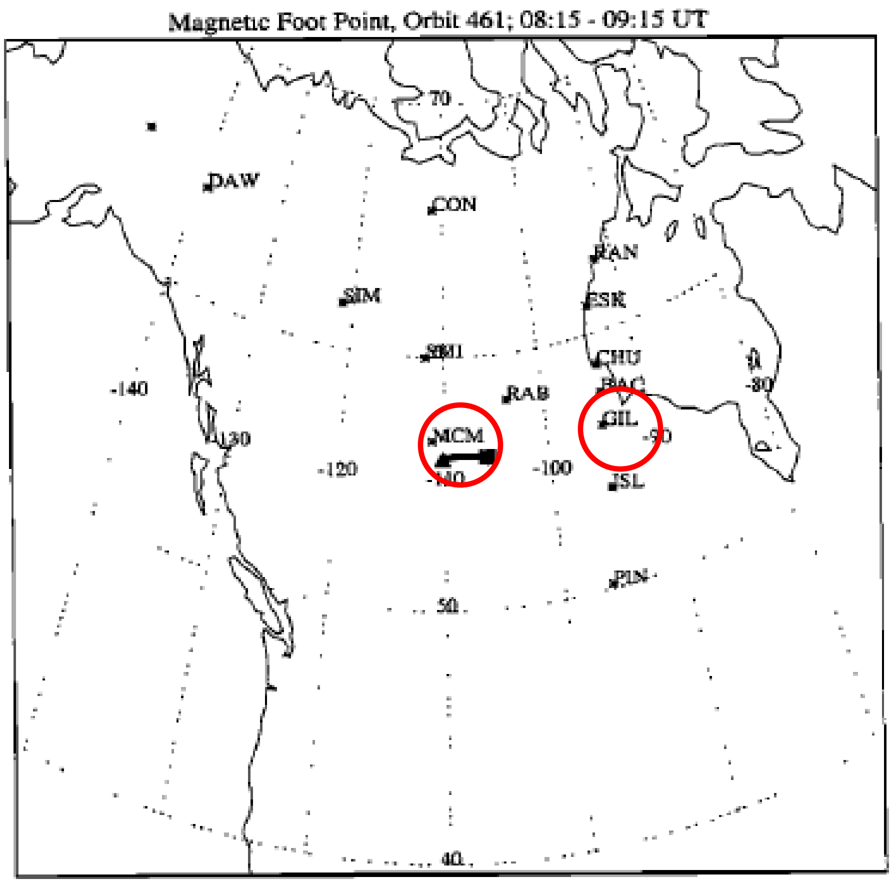

LEXO = local explosive onset
EXP = explosive growth phase

Magnetic Storms and Substorms

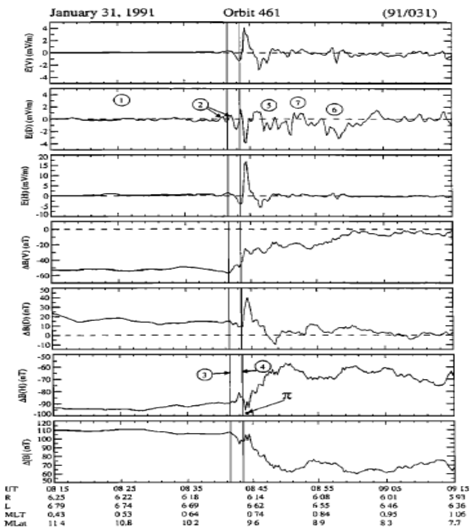

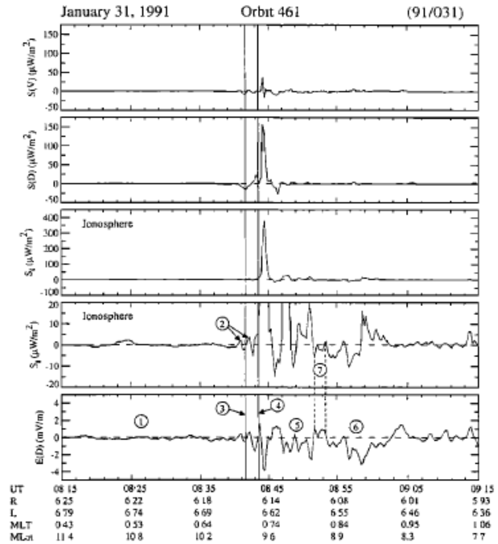

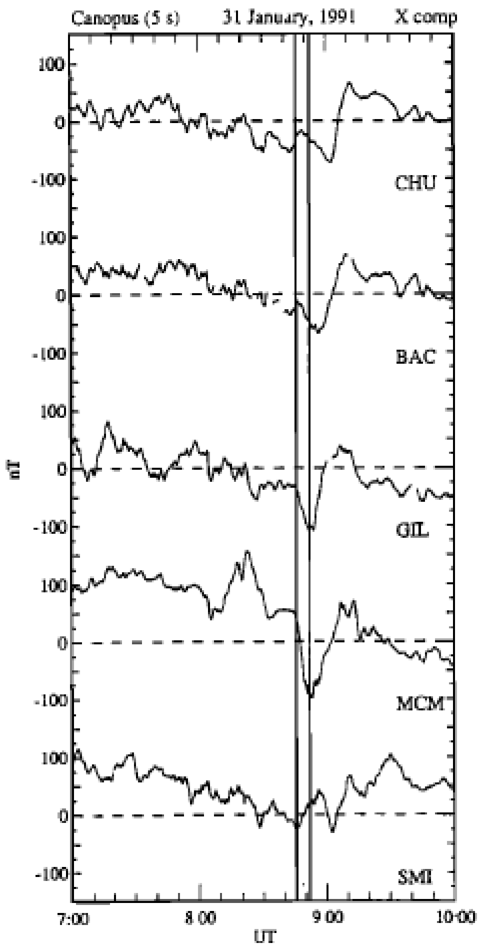

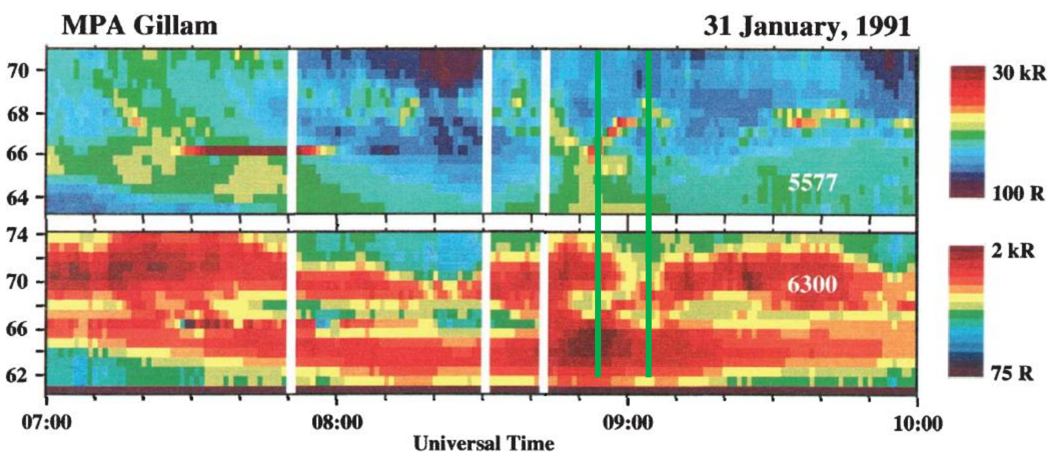

Magnetic Storms and Substorms

The Bottom line:

The substorm problem has been with us for a long time. In the 1970s the concepts of near-Earth neutral-line reconnection and disruption of the cross-tail current sheet were widely discussed.

To this day there are pitched battles between which has precedence in substorm onset.

CRRES data seem to support the substorm current wedge model.

During the growth phase the electric field oscillations have little to no associated magnetic perturbations and no measurable field-aligned currents or Poynting flux. (An electrostatic gradient-drift mode that leaves no foot prints on Earth)

This ends when δE becomes large and $E_{total} = E_0 + \delta E$ turns eastward and $j \cdot E_{total} < 0$. Region becomes a local generator coupling the originally electrostatic to an electromagnetic Alfvén model that carries $j_{||}$ and $S_{||}$ to the ionosphere. Pi 2 waves seen when Alfvén waves reach the ionosphere.

Magnetic Storms and Substorms

McPherron, R. L., C. T. Russell, and M. P. Aubry (1973), Satellite studies of magnetospheric substorms on August 15, 1968: 9. Phenomenological model for substorms, *J. Geophys. Res.*, 78(16), 3131–3149.